A Novel Hybrid Method for Estimating Channel Temperature and Extracting the AlGaN/GaN HEMTs Model Parameters

Mi Zhang, *Student Member, IEEE*, Wenquan Che, *Senior Member, IEEE*, and Kaixue Ma, *Senior Member, IEEE*

***Abstract*— A new hybrid method for estimating channel temperature and extracting the AlGaN/GaN high electron mobility transistors (HEMTs) model parameters is proposed in this paper. The method studies the temperature-dependent feature of access resistances and estimates the channel temperature of tested device by using a novel scanning channel temperature optimization approach. For the first time, the relationship between thermal resistance (R_{th}) and bias voltage is used to ensure the accuracy of the HEMT device model. The estimated channel temperatures are experimentally verified by using the Raman spectroscopy method. For different sizes of the AlGaN/GaN HEMT device, the simulation results based on the proposed model are compared with the conventional model as well as the commercial model, a better agreement with the measurement data for the proposed method is achieved.**

***Index Terms*— Device modeling, GaN, high electron mobility transistors (HEMTs), hybrid extraction method, thermal resistance.**

I. Introduction

AlGaN/GaN high electron mobility transistors (HEMTs) have been widely used in high-power applications and the accuracies of their models can obviously influence the performance of the designed circuits [1]–[3]. Many solutions to extract GaN models were reported in the last decade. Dambrine *et al*. [4] proposed a general step to extract model parameters for GaAs devices, which was then applied as the rationale to solve the GaN modeling problems. It is well known that prevalent GaN modeling method assumes the small signal equivalent circuit can be divided into extrinsic and intrinsic parts, with the extrinsic part parameters fixed, to simplify the modeling problem. Nevertheless, Angelov *et al*. [5] proposed that the values of access resistances, i.e., source resistance (R_s) and drain resistance (R_d), which are the elements of extrinsic parts, will obviously augment under actual device operation bias due to the increasing channel temperature caused by self-heating effect. Therefore, extracting these access resistances from conventionally cold measurements and neglecting the increase of their resistance value would lead to unrealistically optimistic output power and power-added efficiency; similar conclusion was drawn in [6]–[8]. Trew *et al*. [9] verified the existence of a nonlinear source resistance caused by the onset of space-charge-limited current phenomenon. However, Trew's theory [9] is not valid for the small signal condition. On the other hand, the hot-FET method was proposed to solve this problem by using variable extrinsic circuit parameters obtained from optimization [10]. Moreover, Fan *et al*. [1] solved this problem by using a hybrid extraction algorithm combining the cold-FET and hot-FET methods with imposed constraints to avoid negative values. Nevertheless, the deficiency of conventional optimization method used in foregoing works is a starting point related and nonphysical convergence, e.g., overlarge access resistance values or obtained zero values with the constraint condition to avoid negative values.

An electrical method for estimating the channel temperature was investigated in [11] and [12], based on the difference in drain current between dc and short-pulsed conditions. In this paper, the channel temperatures were estimated by calculating the minimum composite error of the equivalent circuit, thus the model accuracy is also improved. A new hybrid method including a multitemperature condition cold-FET method and a scanning channel temperature optimization routine for extracting the AlGaN/GaN HEMTs model parameters is presented in this paper. The channel temperature-dependent extrinsic parts are extracted by using the cold-FET method performed under different ambient temperature conditions. The channel temperatures and corresponding extrinsic parts under each specific actual biased operating condition are estimated by using the method of scanning channel temperature. The method of scanning channel temperature estimates the channel temperature by using an optimization routine to choose minimum composite error of the circuit model. Furthermore, according to the relationship between thermal resistance (R_{th}) and bias [13]–[15], the increased channel temperature is reoptimized to ensure the accuracy. Finally, the Raman spectroscopy method was used to verify the optimized channel temperature.

This paper is organized as follows. In Section II, the hybrid extraction method is described. In Section III, the proposed

Manuscript received January 17, 2018; revised February 13, 2018; accepted February 14, 2018. Date of publication March 6, 2018; date of current version March 22, 2018. This work was supported by the National Natural Science Foundation of China under Grant 61571231 and Grant 61627802. The review of this paper was arranged by Editor G. Verzellesi. *(Corresponding author: Wenquan Che.)*

M. Zhang and W. Che are with the Department of Communication Engineering, Nanjing University of Science and Technology, Nanjing 210094, China (e-mail: yeeren_che@163.com).

K. Ma is with the School of Physics, University of Electronic Science and Technology of China, Chengdu 610054, China (e-mail: makaixue@uestc.edu.cn).

Color versions of one or more of the figures in this paper are available online at http://ieeexplore.ieee.org.

Digital Object Identifier 10.1109/TED.2018.2808267

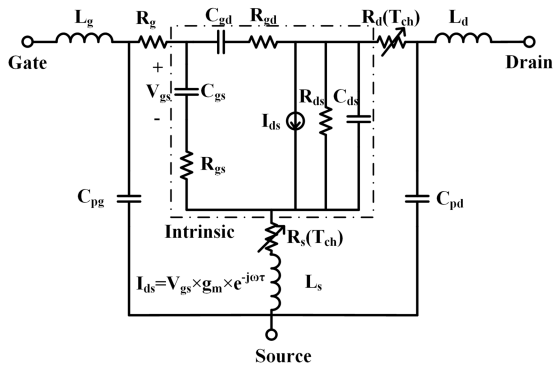

Fig. 1. 16-element temperature-dependent small-signal equivalent circuit of AlGaN/GaN HEMTs.

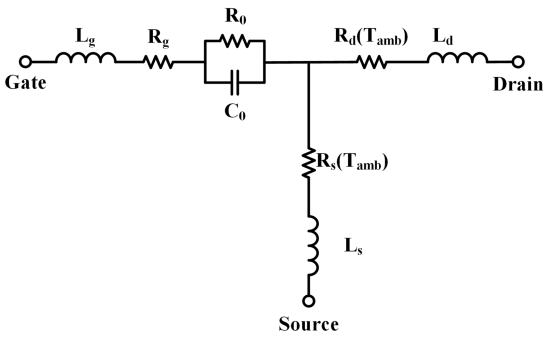

Fig. 2. Equivalent circuit of AlGaN/GaN HEMTs under the condition of low dc forward current and open drain.

extraction method is used to extract parameters of different sizes of the AlGaN/GaN devices. In Section IV, the model results and corresponding channel temperature of proposed extraction method are verified and discussed. Finally, the conclusions are drawn in Section V.

II. Hybrid Extraction Method

The hybrid method combines a multitemperature condition cold-FET method together with a scanning channel temperature optimization routine. A 16-element equivalent circuit model including the channel temperature-dependent parameters of the access resistances R_s ($T_{\rm ch}$) and R_d ($T_{\rm ch}$) in extrinsic parts is employed to imitate the behavior of these devices, as given in Fig. 1. Both the values of R_s ($T_{\rm ch}$) and R_d($T_{\rm ch}$) are extracted using cold-FET measurements at different ambient temperatures. Meanwhile, the other extrinsic parameters, i.e., R_g, L_s, L_d, L_g, $C_{\rm pd}$, and $C_{\rm pg}$, are still assumed to be stable when temperature or bias condition changes. The intrinsic parameters are extracted at different channel temperatures and finally determined by using the scanning channel temperature optimization routine. The extraction of the model parameters will be investigated and discussed in the following.

A. Multitemperature Cold-FET Condition Method

First, to find the relationship between R_s ($T_{\rm ch}$) and R_d ($T_{\rm ch}$) and channel temperature, cold-FET measurements were carried out at different ambient temperatures. Under the conditions such as low dc forward current ($0 < V_{\rm gs} < V_{\rm bi}$, $V_{\rm bi}$ is the built-in voltage; $I_{\rm gs} > 0$), open drain, and the ambient temperature $T_{\rm amb}$, the proposed equivalent circuit is as shown in Fig. 2. The extrinsic parameters are extracted based on the theory in [16]–[18]. The access resistances can be calculated by the real parts of Z-parameters

$$R_s(T_{\rm amb}) = {\rm Re}(Z_{12}) \tag{1}$$

$$R_d(T_{\rm amb}) = {\rm Re}(Z_{22})\text{-}R_s \tag{2}$$

where Z_{12} and Z_{22} are the Z-parameters of cold-FET measurement results.

Under the cold-FET condition, the ambient temperature of the test environment can be considered as the channel temperature after the transistor is uniformly heated. The relationship between access resistances $R_{\rm s}$ ($T_{\rm ch}$) and R_d ($T_{\rm ch}$) and channel temperatures is almost linearly related according to [5]–[8]. Thus, within the safety temperature range, the relationship between access resistance values and channel temperatures can be expressed as follows:

$$R_s(T_{\rm ch}) = R_{\rm s0} + T_{\rm rs} \times T_{\rm ch} \tag{3}$$

$$R_d(T_{\rm ch}) = R_{\rm d0} + T_{\rm rd} \times T_{\rm ch} \tag{4}$$

where R_{s0} and R_{d0} are the drain and source resistances when the channel temperature is 0 °C. $T_{\rm rd}$ and $T_{\rm rs}$ are the coefficients of increase resistance per degree celsius and $T_{\rm ch}$ is the channel temperature of the GaN device. This method assumes that the values of access resistances are related with the channel temperature, and the temperature-distributed effect is negligible for the device channel.

B. Scanning Channel Temperature Optimization Routine

The novel channel temperature scanning method is used to link different bias conditions to their corresponding raised channel temperatures. At each channel temperature, the corresponding channel temperature-dependent extrinsic resistances are calculated using (3) and (4), whereas other extrinsic parameters are fixed. The intrinsic parameters are then extracted based on the de-embedding theory in [4]. Furthermore, the HEMT model can be determined and the model error between simulated and measured result can also be obtained. The error in the proposed model is evaluated by calculating the composite error (ε_0) from the extracted intrinsic Y-parameters' error (ε_1) and the whole model circuit's S-parameters' error (ε_2).

The error of the intrinsic part can be calculated from Y-parameters as follows:

$$\varepsilon_{Y_{ij}} = \sum_{N} \left(\frac{|Y_{ij}^{\rm ext} - Y_{ij}^{de}|^p}{|Y_{ij}^{de}|^p} \right) \Big/ N \tag{5}$$

$$\%\varepsilon_1 = 100 \times \sum_{i,j=1}^{2} \left(w_{Y_{ij}} \times \sqrt[p]{\varepsilon_{Y_{ij}}} \right) \tag{6}$$

where N is the number of the frequency points involved, $Y^{\rm de}$ are the de-embedded intrinsic Y-parameters determined by using the measured complete device S-parameters and extrinsic parts, $Y^{\rm ext}$ are the intrinsic Y-parameters calculated

by using extracted intrinsic parameters, and w_{Yij} is the weight factor of each Y-parameters primitively determined by the normalization error. The value of p is either 1 or 2, which should be determined by using the measurement data; p is equal to 1 in this paper for more tolerance of noise and measurement uncertainty.

The error of the complete device model is calculated using S-parameters as follows:

$$\varepsilon_{S_{ij}^{\text{sim}}} = \sum_{N} \left(\frac{|S_{ij}^{\text{sim}} - S_{ij}^{\text{meas}}|^p}{|S_{ij}^{\text{meas}}|^p} \right) \Big/ N \tag{7}$$

$$\%\varepsilon_2 = 100 \times \sum_{i,j=1}^{2} \left(w_{S_{ij}} \times \sqrt[p]{\varepsilon_{S_{ij}^{\text{sim}}}} \right) \tag{8}$$

where S^{meas} are the measured S-parameters of device under test (DUT), S^{sim} are the S-parameters simulated by using the extracted model, and w_{Sij} is the weight factor of each S-parameter primitively determined by the normalization error in each S-parameter.

Finally, the value of the composite error ε_0 is calculated as follows:

$$\%\varepsilon_0 = w_1 \times \varepsilon_1 + w_2 \times \varepsilon_2 \tag{9}$$

where w_1 and w_2 are the weight factors of the error in the intrinsic Y-parameters and complete device S-parameters. The initial values of w_1 and w_2 are 1, this means that the error of intrinsic Y-parameters and overall S-parameters has equal weight upon the determination of the model.

Moreover, the weight factors in (6) and (8) can be manually modified in order to improve the accuracy of a specific performance, e.g., the model is designed to predict accurate input impedance then the weight factor w_{S11} would be increased, whereas the weight factor w_{S21} would be increased if accurate prediction for gain is required.

Under a certain bias condition, scanning the increased channel temperature from zero to an absolute high temperature can be equivalent to calculate a series of temperature-dependent extrinsic circuits. By de-embedding the intrinsic parts from these extrinsic circuits based on the DUT measurement results, a series of models with different channel temperatures can be obtained. The most appropriate channel temperature value is determined by calculating the composite error (ε_0) of the series of models at different channel temperatures and finding the one with minimum ε_0 in them.

Moreover, the weight factors in (9) can be tuned to guarantee that the obtained R_{th} increases under higher bias voltage, which agrees with the observed results in [13]–[15]. This constraint condition ensures that the optimized channel temperature increases under higher bias and improves the multiple-valued condition of the proposed optimization approach. The R_{th} is calculated as

$$T_{\text{th}} = \Delta T / (I_{\text{ds}} \times V_{\text{ds}}) = \Delta T / P_{\text{dc}} \tag{10}$$

where the ΔT is the raised channel temperature under higher bias, the I_{ds} and V_{ds} are the drain–source current and the drain–source voltage, and P_{dc} is the dc power of operating device.

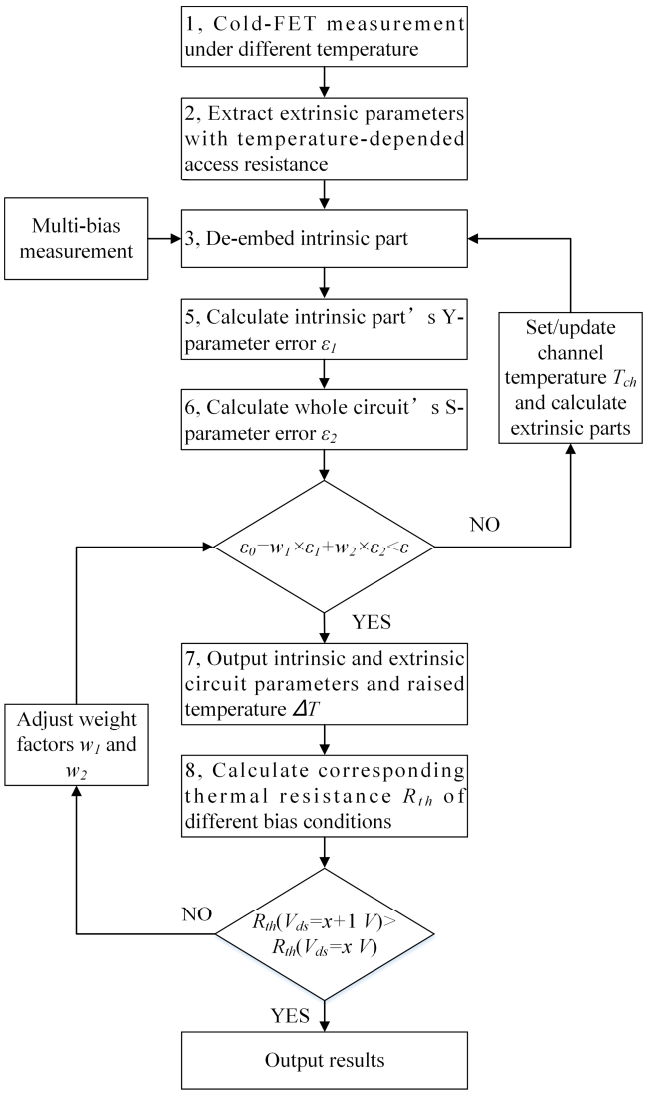

Fig. 3. Flowchart of proposed hybrid extraction method.

The flowchart of the proposed hybrid extraction method is given in Fig. 3. The multitemperature cold-FET condition method is used to obtain channel temperature-dependent access resistances. The initial value of channel temperature is set to be ambient temperature, and the ε_0 of initial channel temperature is calculated. Then, the value of channel temperature is increased by the certain step, and the ε_0 calculation process to find the minimum ε_0 can be done. Furthermore, the estimated channel temperatures are reverified by the values of R_{th}. If the R_{th} increases under higher bias voltage, the optimization process would continue, or else, the program would remodify the composite error equation and execute the error calculation. The output results of the proposed hybrid extraction method include the model parameters and the estimated channel temperatures under different bias conditions.

III. Experimental Model Extraction

The AlGaN/GaN HEMT devices used for extraction method verification in this paper are from WIN Semiconductors Corporation, NP25-00 0.25-μm GaN/SiC HEMT foundry, with similar gate length of 0.25 μm and three different gate widths

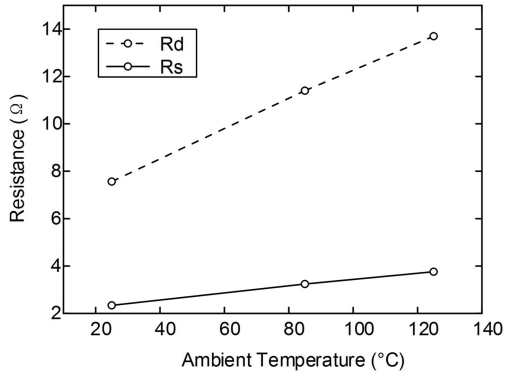

Fig. 4. Source resistance (R_s) and drain resistance (R_d) of a $2\times125\ \mu m^2$ AlGaN/GaN HEMT device as a function of ambient temperature extracted by the cold-FET method.

TABLE I
EXTRINSIC PARAMETERS OF NO-BIAS $2 \times 125\ \mu m^2$ GaN HEMT AT DIFFERENT AMBIENT TEMPERATURES

Extrinsic Parameters at 25 °C							
R_d (Ω)	R_s (Ω)	R_g (Ω)	L_d (pH)	L_g (pH)	L_s (pH)	C_{pg} (fF)	C_{pd} (fF)
7.56	2.34	1.64	58.1	46.9	2.39	115	87.2
Extrinsic Parameters at 85 ° C							
R_d (Ω)	R_s (Ω)	R_g (Ω)	L_d (pH)	L_g (pH)	L_s (pH)	C_{pg} (fF)	C_{pd} (fF)
11.4	3.24	1.67	54.7	48.0	2.23	116	87.9
Extrinsic Parameters at 125 ° C							
R_d (Ω)	R_s (Ω)	R_g (Ω)	L_d (pH)	L_g (pH)	L_s (pH)	C_{pg} (fF)	C_{pd} (fF)
13.7	3.74	1.73	52.5	50.4	2.15	118	88.7
Relatively change from 25 ° C to 125 ° C							
81.2 %	59.8 %	5.5 %	-9.6 %	7.5 %	-10 %	2.6 %	1.7 %

of $2 \times 50\ \mu m^2$, $2 \times 75\ \mu m^2$, and $2 \times 125\ \mu m^2$. The model parameters of these HEMTs are extracted by the above-mentioned process.

A. Extrinsic Parameters Extraction

Taking the GaN device with gate length of 0.25 μm and gate widths of $2 \times 125\ \mu m^2$ as an example, the relationship between access resistance values and ambient temperatures is given in Fig. 4. These data are obtained by carrying out the cold-FET measurement method at 25 °C, 85 °C, and 125 °C, respectively. According to the previous works in [5]–[8], the relationship between access resistance values and ambient temperature conditions is almost linear, which can be expressed as follows:

$$R_d = 6.03 + 0.0614 \times T_{\rm ch} \tag{11}$$

$$R_s = 1.99 + 0.0142 \times T_{\rm ch}. \tag{12}$$

The measurement data series for different ambient temperatures are only three, but still enough to describe the linear change of access resistances, and the following process performs well with these expressions.

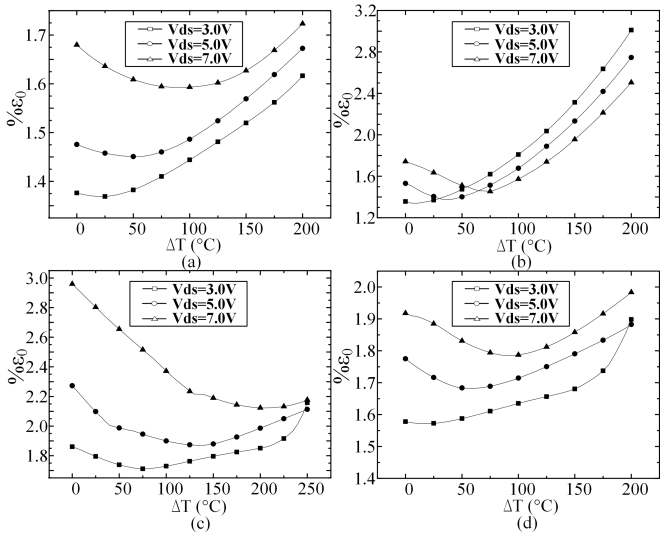

Fig. 5. Relationship between composite error ε_0 result and raised temperature. (a) $2 \times 50\ \mu m^2$ GaN HEMTs under $V_{gs} = -1.5$ V. (b) $2\times75\ \mu m^2$ GaN HEMTs under $V_{gs} = -1.5$ V. (c) and (d) $2\times125\ \mu m^2$ GaN HEMTs under $V_{gs} = -1$ V and $V_{gs} = -2$ V.

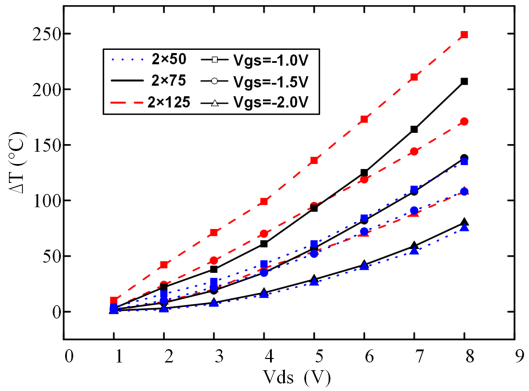

Fig. 6. Relationship between raised temperature and bias conditions in cases of three 0.25-μm GaN HEMTs with gate width of $2 \times 50\ \mu m^2$, $2 \times 75\ \mu m^2$, and $2 \times 125\ \mu m^2$.

The other extrinsic parameters are extracted, and the measurement results at different ambient temperatures are given in Table I. The values of R_s and R_d change by 59.8% and 81.2%, respectively, and the values of other extrinsic parameters change by less than 13% when the temperature rises from 25 °C to 125 °C.

B. Model Parameters Determination by Using Scanning Channel Temperature Optimization Routine

The novel scanning channel temperature optimization routine is used to link different bias conditions with their corresponding raised channel temperatures by calculating the minimum composite error. In Fig. 5, the relationship between composite error and estimated raised channel temperature (ΔT) is given, which shows that by scanning ΔT from 0 °C to 300 °C, the model error can reach a minimum value at the optimized channel temperature. By using the optimized access resistances in the extrinsic parts, the errors of extracted intrinsic part and also the whole circuit model can be reduced. In addition, Fig. 5

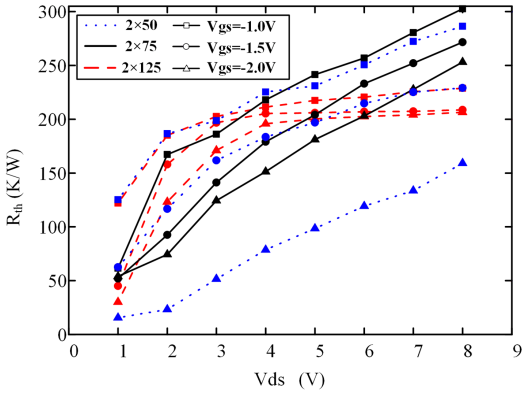

Fig. 7. Relationship between R_{th} and bias conditions in cases of three 0.25-μm GaN HEMTs with gate width of 2×50 μm^2, 2×75 μm^2, and 2×125 μm^2.

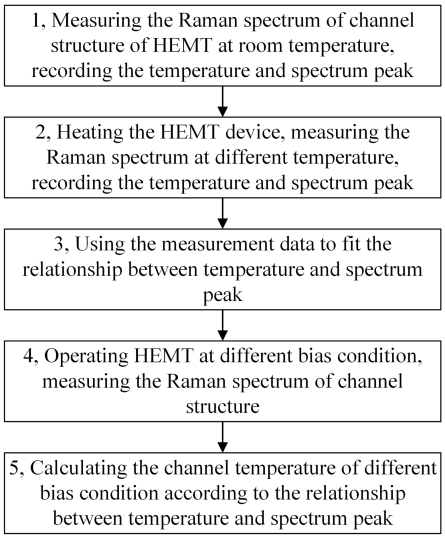

Fig. 8. Measurement steps of the Raman spectroscopy method.

shows that ΔT increases at higher biased voltage. Fig. 6 shows the relationship between raised channel temperature and bias voltage obtained by using the approach of scanning channel temperature. As to the measurement data, the drain–source current I_{ds} is negligible at the bias of $V_{\text{gs}} = -2$ V and $V_{\text{ds}} = 1$ V; therefore, the small ΔT of these bias points is reasonable.

The value of R_{th} is calculated by using (10). Fig. 7 shows the relationship between R_{th} and bias conditions, which are in accordance with that the R_{th} increases under higher bias voltage. The output values are calculated in accordance with the positive correlation between bias and R_{th}. From (10), as the dc power of these devices is small, typically less than 1 W, the R_{th} changes significantly when the channel temperatures change. Especially when $V_{\text{ds}} = 1$ V, the dc power is a few milliwatts, so the estimated R_{th} are not precise, however, the monotonic raise with bias increase could be observed.

IV. Model Validation and Discussion

The estimated channel temperatures are verified by using the Raman spectroscopy method [19]. The Raman measurements were performed with Renishaw's inVia Raman spectrometer

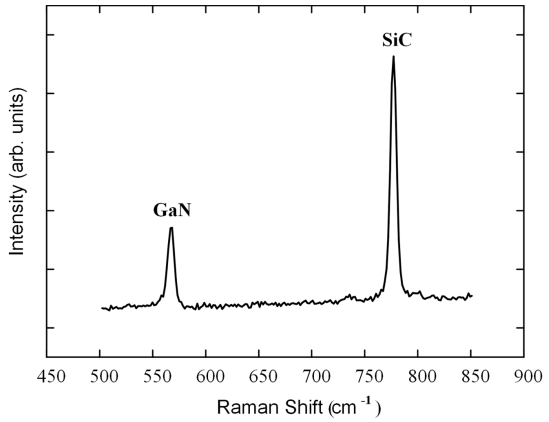

Fig. 9. Raman spectrum of GaN HEMT channel structure without bias at 25 °C.

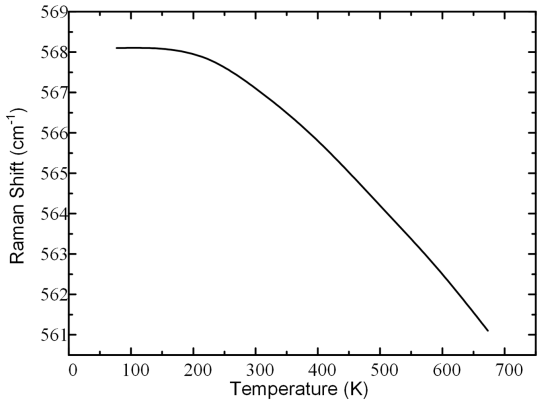

Fig. 10. Relationship between the channel temperature and the Raman shift.

using a 514-nm laser. The laser beam was focused on the gate finger in the middle of active region in a spot with diameter less than 1 μm. Determination of the temperature by Raman spectroscopy is based on the fact that different substances have different spectra; however, when the temperature of certain substance rises, the Raman shift of spectrum peak reduces. The measurement steps of the Raman spectroscopy method are given in Fig. 8. First, the Raman shift of unbiased HEMT is measured at different temperatures. Fig. 9 shows a Raman spectrum of channel structure without bias at 25 °C, the Raman shift of GaN is around 567 cm^{-1}, and the Raman shift of SiC is around 778 cm^{-1}. The relationship between temperature and spectrum peak is fit using the measurement data of the Raman shift at different temperatures, which is shown in Fig. 10. By operating the HEMT at different bias conditions and measuring the Raman spectrum of channel structure, the channel temperatures under different bias conditions are calculated. Fig. 11 shows the comparison between the measured and estimated channel temperatures of 0.25-μm GaN HEMT with 2×125 μm^2 gate width, which implies that the proposed method could approximately estimate the channel temperatures. However, the estimated channel temperatures at $V_{\text{gs}} = -2.0$ V are somewhat lower than the measurement results, probably because the raised channel temperatures are low and the increase of access resistances is not significant.

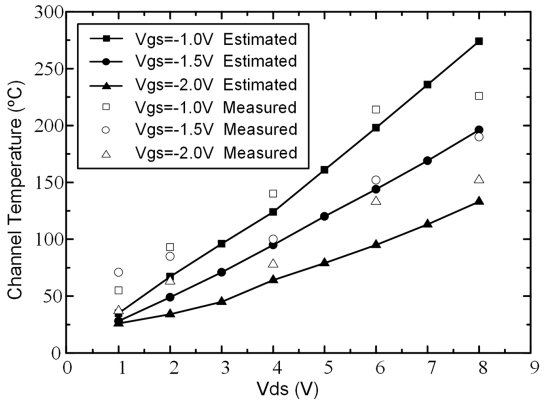

Fig. 11. Comparison between measured channel temperatures and estimation channel temperatures of 0.25-μm GaN HEMT with 2×75 μm^2 gate width.

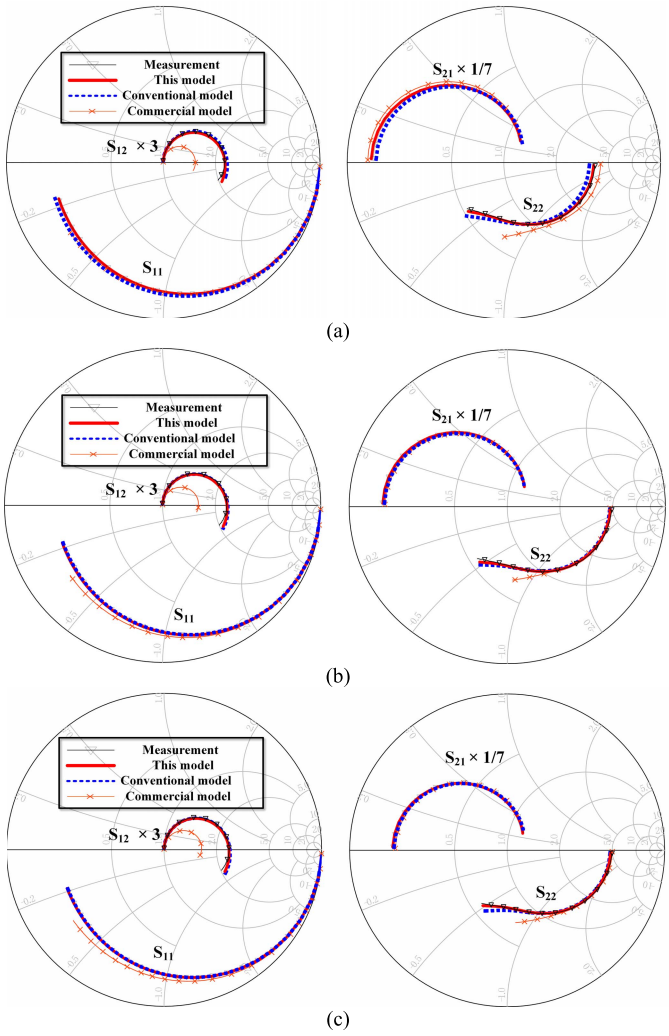

Fig. 12. Comparison between the measurement (black triangle line), this model (red solid line), conventional model (blue dotted line), and the commercial model (orange X line) S-parameters for a 0.25-μm GaN HEMT with 2×125 μm^2 gate width at $V_{gs}=-1.5$ V and $V_{ds}=5$ V for 0.1–20.1 GHz at (a) 25 °C, (b) 85 °C, and (c) 125 °C.

The proposed hybrid extraction method is also verified through the small signal model S-parameter measured and simulated at different ambient temperatures from 0.1 to 20.1 GHz.

TABLE II
QUANTIZED S-PARAMETER ERRORS OF THREE MODELS AT THE BIAS OF $V_{gs}=-1.5$ V AND $V_{ds}=5$ V OVER 25 °C FOR THREE SIZES OF GaN HEMT

0.25-μm GaN HEMT with 2 × 50 μm gate width		
	This Work	Conventional Model
%εS11	**0.88**	1.08
%εS12	**2.35**	3.26
%εS21	**0.91**	1.45
%εS22	**0.39**	4.63
%εStotal	**4.53**	10.42
0.25-μm GaN HEMT with 2 × 75 μm gate width		
	This Work	Conventional Model
%εS11	**0.34**	0.49
%εS12	**2.02**	2.13
%εS21	**0.49**	3.26
%εS22	**2.00**	5.64
%εStotal	**4.85**	11.52
0.25-μm GaN HEMT with 2 × 125 μm gate width		
	This Work	Conventional Model
%εS11	**0.30**	2.41
%εS12	**2.69**	6.06
%εS21	**1.08**	2.94
%εS22	**1.91**	6.43
%εStotal	**5.98**	17.84

In Fig. 12, under the bias condition of $V_{gs}=-1.5$ V and $V_{ds}=5$ V at temperature of 25 °C, 85 °C, and 125 °C, respectively, the S-parameters based on the proposed model are compared with the measured S-parameters, the model results of a conventional parameter extraction process without temperature-dependent extrinsic parts, and the commercial model provided by WIN Semiconductors Corporation, respectively. The S-parameters obtained from the proposed model agree well with the measurement data, and the coincidence of the proposed model results to the measurement results is better than that of the other two models. Moreover, to further demonstrate the validity of our proposed model, the quantized S-parameter errors are calculated by using the error expression in [20]. Table II lists the quantized S-parameter errors of this model and the conventional model for GaN HEMTs of three sizes (0.25-μm GaN HEMTs with 2×50 μm^2, 2×75 μm^2, and 2×125 μm^2 gate width) at the bias of $V_{gs}=-1.5$ V and $V_{ds}=5$ V at 25 °C. For 2×50 μm^2 HEMT, the total error in S-parameters (%εStotal) in this paper is 4.63%, which is 5.89% less than that of the conventional model. As for the 2×75 μm^2 HEMT, the %εStotal in this paper is 4.85%, which is 6.67% less than that of the conventional model. For 2×125 μm^2 HEMT, the %εStotal in this paper is 5.98%, which is 11.86% less than that of the conventional model. It can be concluded that the proposed model has better accuracy. The high V_{gs} bias

conditions are chosen for validation, because the I_{ds} are much higher at high V_{gs} biases than at high V_{ds} biases. Therefore, the thermal effect is more significant at high V_{gs} biases.

V. Conclusion

A novel hybrid method for extracting the AlGaN/GaN HEMTs model parameters is presented. The method solves the unrealistic performance prediction problem caused by the fixed R_s and R_d of conventional models. Channel temperature-dependent R_s and R_d are obtained from the cold-FET measurement implemented under different ambient temperature conditions, and the channel temperature of operating device is obtained by scanning channel temperature method. The optimized channel temperatures are experimentally verified by using the Raman spectroscopy method. The modification on R_s and R_d may cause a little complexity in extraction process, but model accuracy can be obviously improved. The proposed method can be used to estimate the channel temperature and provides an efficient way to investigate the relationship between channel temperature and whole model parameters. Moreover, the reliability of this method for multifinger devices still requires further verification. Furthermore, the accurate nonlinear parameters extracted by our method can be used to develop a large signal HEMT model in our following work.

Acknowledgment

The authors would like to thank Dr. I. Angelov, Chalmers University of Technology, Göteborg, Sweden, for his helpful discussions on temperature-dependent access resistances and the model parameter extraction method.

References

[1] F. Qian, J. H. Leach, and H. Morkoc, "Small signal equivalent circuit modeling for AlGaN/GaN HFET: Hybrid extraction method for determining circuit elements of AlGaN/GaN HFET," *Proc. IEEE*, vol. 98, no. 7, pp. 1140–1150, Jul. 2010, doi: 10.1109/JPROC.2010.2044630.

[2] P. Regoliosi *et al.*, "Experimental validation of GaN HEMTs thermal management by using photocurrent measurements," *IEEE Trans. Electron Devices*, vol. 53, no. 2, pp. 182–188, Feb. 2006, doi: 10.1109/TED.2005.862247.

[3] L. Brunel, B. Lambert, D. Carisetti, N. Malbert, A. Curutchet, and N. Labat, "Electrical runaway in AlGaN/GaN HEMTs: Physical mechanisms and impact on reliability," *IEEE Trans. Electron. Devices*, vol. 64, no. 4, pp. 1548–1553, Apr. 2017, doi: 10.1109/TED.2017.2669368.

[4] G. Dambrine, A. Cappy, F. Heliodore, and E. Playez, "A new method for determining the FET small-signal equivalent circuit," *IEEE Trans. Microw. Theory Techn.*, vol. 36, no. 7, pp. 1151–1159, Jul. 1988, doi: 10.1109/22.3650.

[5] I. Angelov *et al.*, "On the large-signal modeling of high power AlGaN/GaN HEMTs," in *IEEE MTT-S Int. Microw. Symp. Dig.*, Montreal, QC, Canada, Jun. 2012, pp. 1–3, doi: 10.1109/MWSYM.2012.6258335.

[6] M. Thorsell, K. Andersson, M. Fagerlind, M. Sudow, P. A. Nilsson, and N. Rorsman, "Thermal study of the high-frequency noise in GaN HEMTs," *IEEE Trans. Microw. Theory Techn.*, vol. 57, no. 1, pp. 19–26, Jan. 2009, doi: 10.1109/TMTT.2008.2009084.

[7] R. J. T. Simms, J. W. Pomeroy, M. J. Uren, T. Martin, and M. Kuball, "Channel temperature determination in high-power AlGaN/GaN HFETs using electrical methods and Raman spectroscopy," *IEEE Trans. Electron Devices*, vol. 55, no. 2, pp. 478–482, Feb. 2008, doi: 10.1109/TED.2007.913005.

[8] A. Inoue *et al.*, "A nonlinear drain resistance model for a high power millimeter-wave PHEMT," in *IEEE MTT-S Int. Microw. Symp. Dig.*, San Francisco, CA, USA, Jun. 2006, pp. 647–650, doi: 10.1109/MWSYM.2006.249697.

[9] R. J. Trew, Y. Liu, G. L. Bilbro, W. Kuang, R. Vetury, and J. B. Shealy, "Nonlinear source resistance in high-voltage microwave AlGaN/GaN HFETs," *IEEE Trans. Microw. Theory Techn.*, vol. 54, no. 5, pp. 2061–2067, May 2006, doi: 10.1109/TMTT.2006.873627.

[10] D. W. DiSanto and C. R. Bolognesi, "At-bias extraction of access parasitic resistances in AlGaN/GaN HEMTs: Impact on device linearity and channel electron velocity," *IEEE Trans. Electron Devices*, vol. 53, no. 12, pp. 2914–2919, Dec. 2006, doi: 10.1109/TED.2006.885663.

[11] S. Martin-Horcajo, A. Wang, M.-F. Romero, M. J. Tadjer, and F. Calle, "Simple and accurate method to estimate channel temperature and thermal resistance in AlGaN/GaN HEMTs," *IEEE Trans. Electron Devices*, vol. 60, no. 12, pp. 4105–4111, Dec. 2013, doi: 10.1109/TED.2013.2284851.

[12] M. A. Alim, A. A. Rezazadeh, and C. Gaquiere, "Temperature effect on DC and equivalent circuit parameters of 0.15-μm gate length GaN/SiC HEMT for microwave applications," *IEEE Trans. Microw. Theory Techn.*, vol. 64, no. 11, pp. 3483–3491, Nov. 2016, doi: 10.1109/TMTT.2016.2604815.

[13] O. Arenas *et al.*, "Electrothermal mapping of AlGaN/GaN HEMTs using microresistance thermometer detectors," *IEEE Electron Device Lett.*, vol. 36, no. 2, pp. 111–113, Feb. 2015, doi: 10.1109/LED.2014.2379213.

[14] B. M. Paine, T. Rust, and E. A. Moore, "Measurement of temperature in GaN HEMTs by gate end-to-end resistance," *IEEE Trans. Electron. Devices*, vol. 63, no. 2, pp. 590–597, Feb. 2016, doi: 10.1109/TED.2015.2510610.

[15] A. Sarua *et al.*, "Thermal boundary resistance between GaN and substrate in AlGaN/GaN electronic devices," *IEEE Trans. Electron Devices*, vol. 54, no. 12, pp. 3152–3158, Dec. 2007, doi: 10.1109/MMM.2008.931675.

[16] A. Z.-D. Landa, J. E. Zuniga-Juarez, J. R. Loo-Yau, J. A. Reynoso-Hernandez, M. D. C. Maya-Sanchez, and J. L. D. Valle-Padilla, "Advances in linear modeling of microwave transistors," *IEEE Microw. Mag.*, vol. 10, no. 2, pp. 100102–111146, Apr. 2009, doi: 10.1109/MMM.2008.931675.

[17] A. Jarndal and G. Kompa, "A new small-signal modeling approach applied to GaN devices," *IEEE Trans. Microw. Theory Techn.*, vol. 53, no. 11, pp. 3440–3448, Nov. 2005, doi: 10.1109/TMTT.2005.857332.

[18] A. E. Parker and S. J. Mahon, "Robust extraction of access elements for broadband small-signal FET models," in *IEEE MTT-S Int. Microw. Symp. Dig*, Jun. 2007, pp. 783–786, doi: 10.1109/MWSYM.2007.380057.

[19] A. Sarua *et al.*, "Integrated micro-Raman/infrared thermography probe for monitoring of self-heating in AlGaN/GaN transistor structures," *IEEE Trans. Electron Devices*, vol. 53, no. 10, pp. 2438–2447, Oct. 2006, doi: 10.1109/TED.2006.882274.

[20] R. G. Brady, C. H. Oxley, and T. J. Brazil, "An improved small-signal parameter-extraction algorithm for GaN HEMT devices," *IEEE Trans. Microw. Theory Techn.*, vol. 56, no. 7, pp. 1535–1544, Jul. 2008, doi: 10.1109/TMTT.2008.925212.

Mi Zhang (S'17) received the B.S. degree from the Nanjing University of Science and Technology, Nanjing, China, in 2013, where he is currently pursuing the Ph.D. degree with the Department of Communication Engineering.

His current research interests include GaN HEMT model and power amplifier design.

Wenquan Che (M'01–SM'11) received the Ph.D. degree from the City University of Hong Kong, Hong Kong.

She is currently a Professor with the Nanjing University of Science and Technology, Nanjing, China. Her current research interests include microwave circuits and medical application of microwave technology.

Dr. Che is an AdCom Member of the IEEE MTT-S.

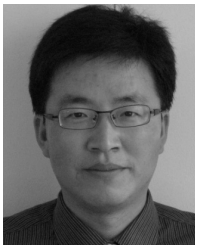

Kaixue Ma (M'05–SM'09) received the Ph.D. degree from Nanyang Technological University (NTU), Singapore.

He was with the China Academy of Space Technology, Xi'an, China, MEDs Technologies, Singapore, ST Electronics, Singapore, and NTU. He is currently a Professor with the University of Electronic Science and Technology, Chengdu, China.

Dr. Ma is named in the China Thousand Talent Program in 2012 and The National Distinguished Young Scholars in 2016.